# Supporting information

## Improving the catalytic performance of cobalt for CO preferential oxidation by stabilizing the active phase through vanadium promotion

Liping Zhong,[a] Mathias Barreau,[a] Valérie Caps,[a] Vasiliki Papaefthimiou,[a] Michael Haevecker,[b,c] Detre Teschner,[b,c] Walid Baaziz,[d] Elisa Borfecchia,[e] Luca Braglia,[f] Spyridon Zafeiratos[a,*]

[a]*Institut de Chimie et Procédés pour l'Energie, l'Environnement et la Santé (ICPEES), ECPM, UMR 7515 CNRS – Université de Strasbourg, 25 rue Becquerel, 67087 Strasbourg Cedex 02, France*

[b]*Max-Planck-Institut für Chemische Energiekonversion (MPI-CEC), Stiftstrasse 34-36, D-45470 Mülheim a.d. Ruhr, Germany*

[c] *Fritz-Haber-Institut der Max-Planck-Gesellschaft, Faradayweg 4-6, D-14195 Berlin, Germany*

[d]*Institut de Physique et Chimie des Matériaux de Strasbourg (IPCMS), UMR 7504 CNRS – Université de Strasbourg, 23 rue du Loess BP 43, 67034 Strasbourg cedex 2, France*

[e]*Department of Chemistry, INSTM Reference Center and NIS Centers, University of Torino, Via P. Giuria 7, 10125 Torino, Italy*

[f]*CNR-IOM, TASC Laboratory, S.S. 14 km 163.5, 34149 Trieste, Italy*

*spiros.zafeiratos@unistra.fr*

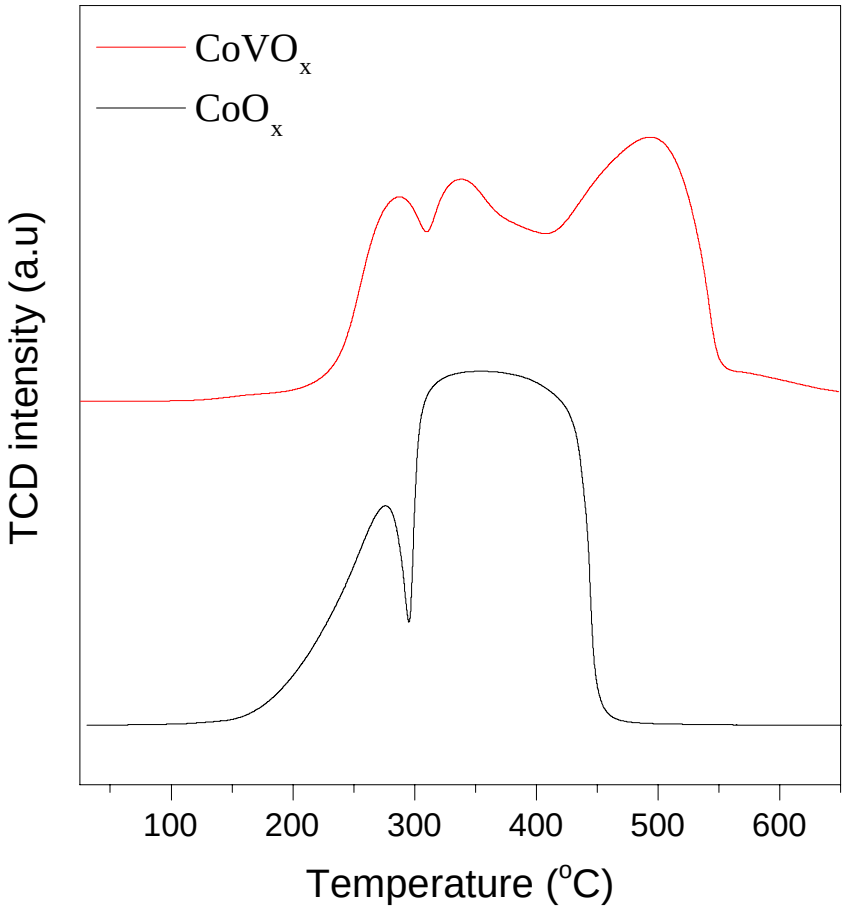


Figure S1: $H_2$-TPR profiles of $CoVO_x$ and CoO catalysts after calcination in air 400°C 3h.

Methane was detected in the products at reaction temperatures of 250 °C and above. The selectivity of CO conversion to $CH_4$ was calculated according to the formula :

$$S_{CH4,T}(\%) = \frac{A_{CH4,T} RF_{CH4}}{A_{CH4,T} RF_{CH4} + A_{CO2,T} RF_{CO2}} \times 100$$

*where*: $A_{i,T}$ are the areas of the corresponding GC peaks at a given reaction temperature T (i=$CH_4$ or $CO_2$). $RF_i$ is the response factor of the gas i (i=$CH_4$ or $CO_2$) determined by external calibration. The evolution of $S_{CH4}$ as a function of the reaction temperature for the two catalysts is shown in Figure S2. It is clear that $CH_4$ selectivity is 0% up to 200 °C but at higher temperatures it increases considerably for both catalysts. The $CoVO_x$ catalyst appears more selective to $CH_4$ than $CoO_x$. The main production path of $CH_4$ is CO hydrogenation reaction (reaction 1). Although contribution of $CO_2$ hydrogenation (reaction 2) cannot be excluded, it is less probable than reaction 1, since CO hydrogenation is more favorable than that of $CO_2$.[1]

*CO hydrogenation:* $CO + 3\,H_2 \rightarrow CH_4 + H_2O$ (1)

*$CO_2$ hydrogenation:* $CO_2 + 4\,H_2 \rightarrow CH_4 + 2\,H_2O$ (2)

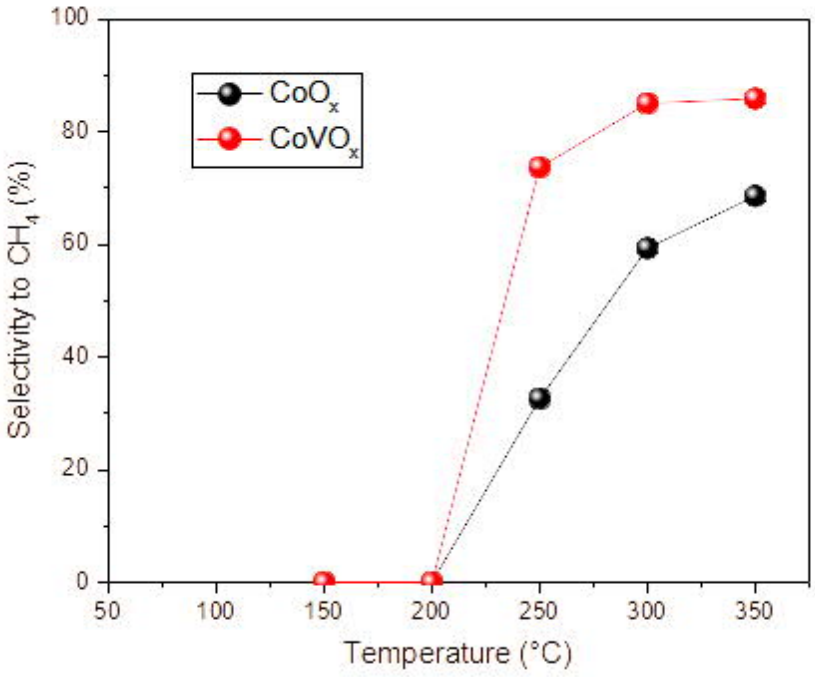


Figure S2: Selectivity to $CH_4$ as a function of temperature for $CoO_x$ and $CoVO_x$ catalysts, based on gas chromatography (GC) measurements. The tests were performed in a fixed bed reactor in 1%CO, 1%$O_2$ and 50%$H_2$ in He-balanced flow; 50 mg of catalyst; 50ml/min of total flow at atmospheric pressure. Each point was recorded after dwell of 30 min at each temperature.

Enhancement of $CH_4$ production with temperature is a well known feature of COPrOx reaction.[2–4] Apart from temperature, $CH_4$ production is influenced by the oxidation state of cobalt and the abundance of adsorbed hydroxyl groups. In particular, $CH_4$ production is promoted on reduced

cobalt catalysts[3,5] and in the presence of high amounts of OH groups.[6] The NAP-XPS results presented in the main text of the paper show that above 250 °C the $CoO_x$ catalyst is in general more oxidized than $CoVO_x$, however it contains higher contribution of OH groups as shown by the high binding energy O 1s component. Unfortunately, the interplay between various factors (temperature, cobalt oxidation state and adsorbed hydroxyl species) does not allow a comprehensive understanding of vanadium effect on $CH_4$ production.

## Supporting information 3: Reactivity of pure V oxide

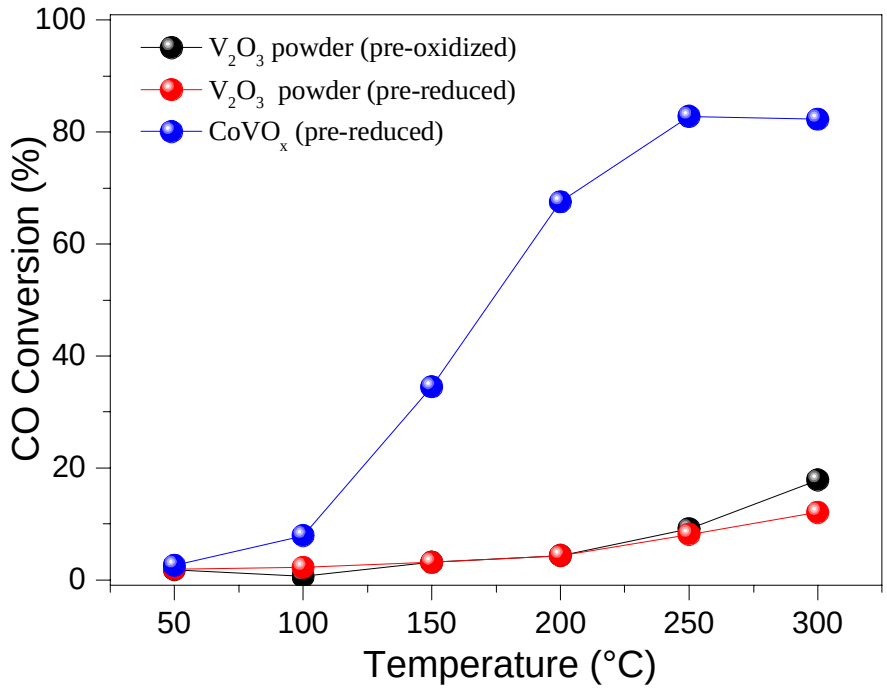


Figure S3: CO conversion of $H_2$ pre-treated $CoVO_x$, $H_2$ pre-treated $V_2O_3$ and $O_2$ pre-treated $V_2O_3$ as a function of temperature, based on gas chromatography (GC) measurements. The reaction was performed in a DRIFT reactor/cell. Experimental Conditions: 1%CO, 1%$O_2$ and 70% $H_2$ in He-balanced flow; 0.11 g catalysts; 10ml/min of total flow; atmospheric pressure (1 bar). Each point was recorded after dwell of 30 min at each temperature.

## Supporting information 4: XRD

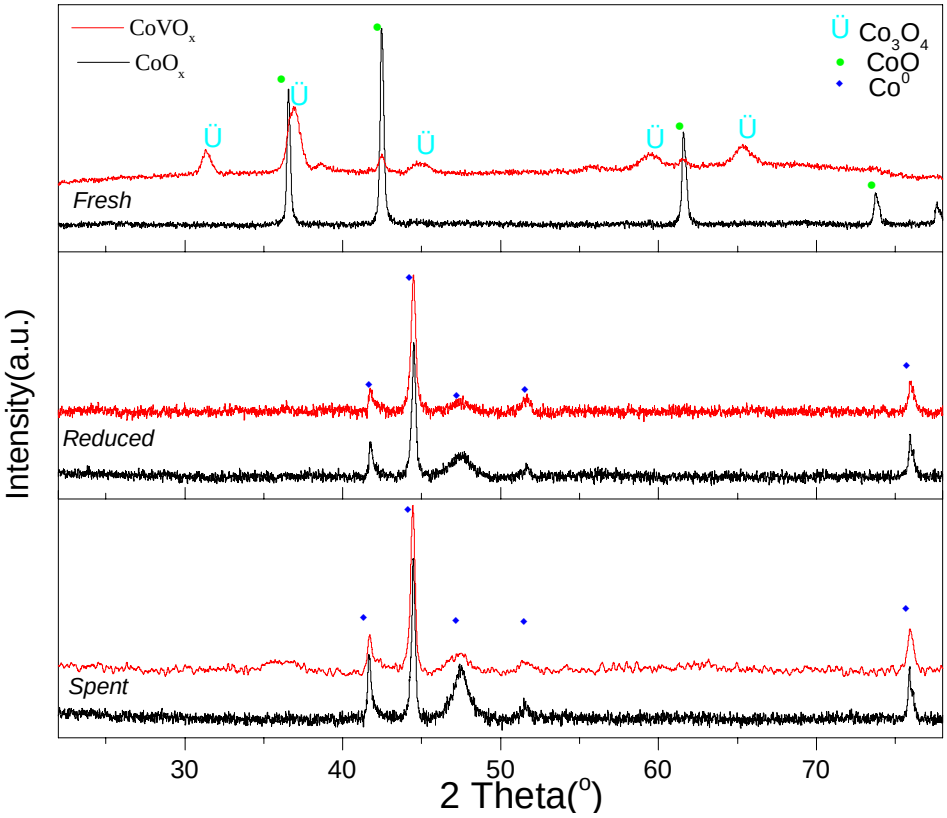


Figure S4. The *ex situ* XRD patterns of fresh (top) reduced (middle) and spent (bottom) $CoO_x$ and $CoVO_x$ catalysts treated at atmospheric pressure conditions.

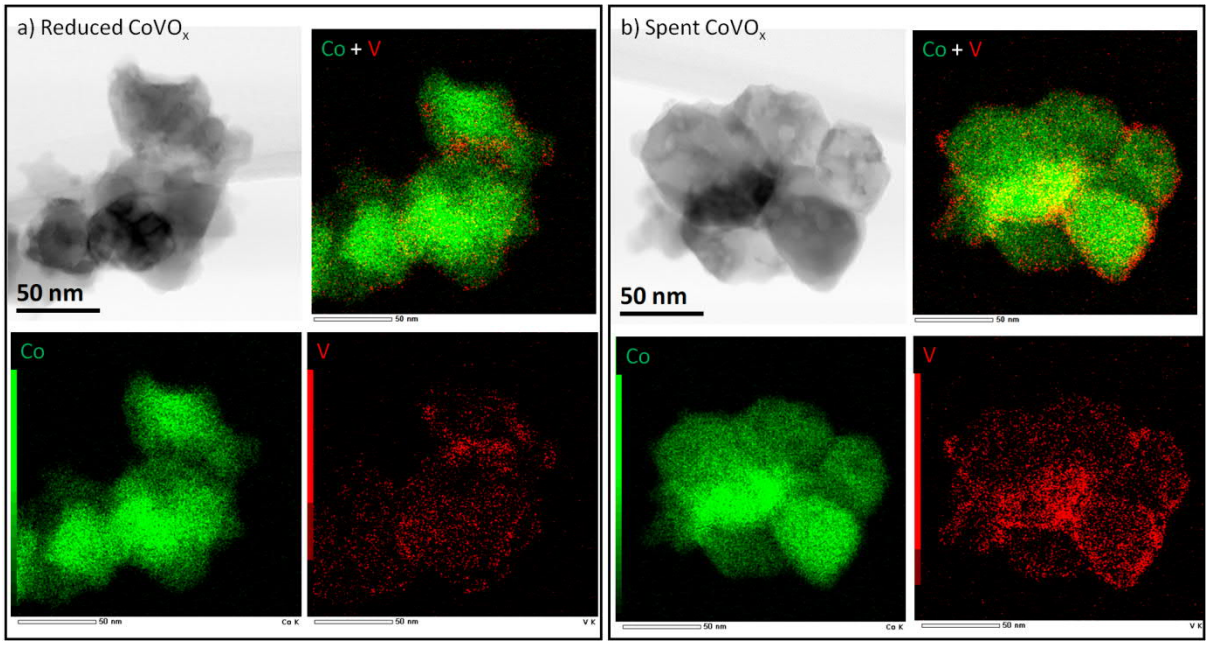


Figure S5a. Representative BF-STEM and the corresponding STEM-EDS analysis images with elemental mapping (Co and V) of a) reduced and b) spent $CoVO_x$ catalyst. Merged images of Co and V maps are shown. Scale bar, 50 nm.

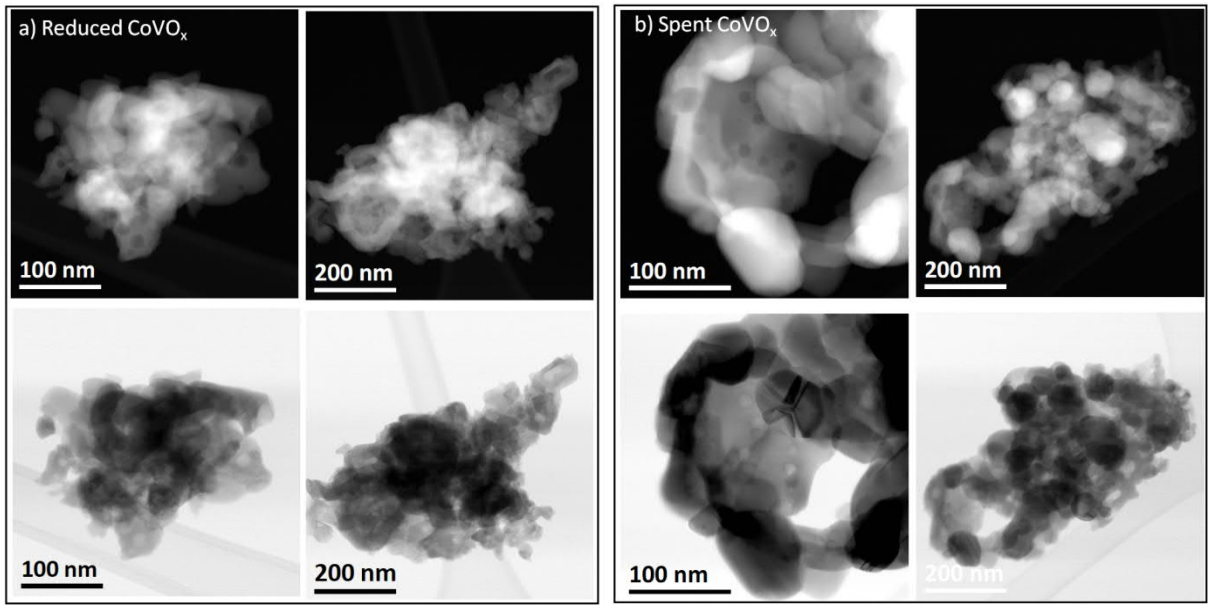


Figure S5b. Representative HAADF-STEM and the corresponding ABF-STEM images of a) reduced and b) spent $CoVO_x$ catalyst.

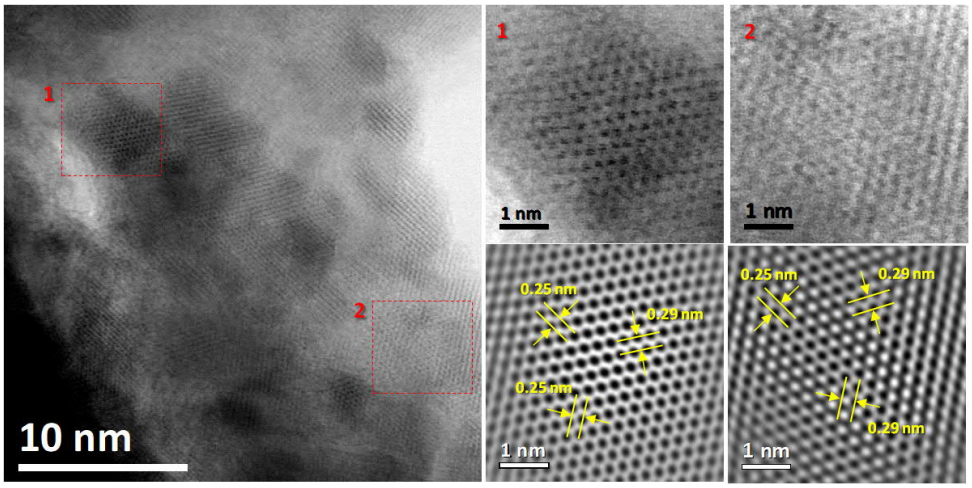


Figure S5c. High resolution BF STEM and the corresponding FFT filtered images (bottom-right) of spent $CoVO_x$ catalysts derived from catalyst areas close to the particles edge. The interplanar spacing is indicated by two parallel lines. The squares indicate the part of the low magnification image from which the high-resolution images are derived.

## Supporting information 6: Co 2p fitting procedure

Photoemission peaks with complex line profiles, like the Co 2p spectra in their various oxidation states, can be fitted using two main approaches. The first involves the use of a synthetic line-shape defined by a combination of individual Voigt–type peaks, each one of them corresponds to a photoemission or a satellite peak which cannot be resolved in the Co 2p spectrum.[7] To avoid over-interpretation, the experimental spectrum should be fitted by using the minimum number of peaks applying several constrains between them. These constrains include, definition of the peak shape, relative position, width and intensity ratio.[7,8]

Alternatively, in case that reference materials are available, it is easier to fit the overall spectrum by using a linear combination of peak line-shapes predefined (measured under identical recording conditions) on the reference components.[8,9] In this latter case the fitting procedure is simplified since considerably lower amount of peaks are used. For example in the case that CoO and $Co_3O_4$ coexist, the overall Co 2p spectrum should be fitted using 18 individual peaks according to the approach described by Biesinger et al,[10] while only 2 peaks are needed (one of each cobalt oxide) when reference peaks from CoO and $Co_3O_4$ are available.[9] Please note that this approach is still credible even if reference spectra contain a small contribution of different cobalt oxidation states. In this case errors in the reference spectra will bring a systematic error in the estimation of average cobalt oxidation state. Systematic errors are less critical when catalysts are evaluated in a comparative basis, like in the present study.

In this work the Co 2p spectra were fitted using line shapes recorded on reference materials (second

approach) using CASA XPS vs 2.3.23 software. The reference peak of metallic Co ($Co^0$) was collected on fully reduced cobalt powder in $H_2$ ambient, those of CoO on reduced cobalt exposed in COPrOx mixture at 150 °C, while the $Co_3O_4$ on cobalt powders under $O_2$ ambient at 350 °C. The acquisition parameters (photon energy, pass energy, and energy step) were kept identical to those of the standard samples. During fitting, the full width at the half maximum and the energy difference between the three reference peaks were fixed. The absolute binding energy and intensity (area) of each peak were allowed to vary until the difference between their sum and the experimental spectrum (residual standard deviation, STD) was minimized (typically between 0.8 and 1.6). The background subtraction was performed using a flexible background shape based on Cubic Spline Polynomials (spline linear profile) which was allowed to adapt for the eventual differences in the background profiles between reference peaks and spectra of the catalysts.

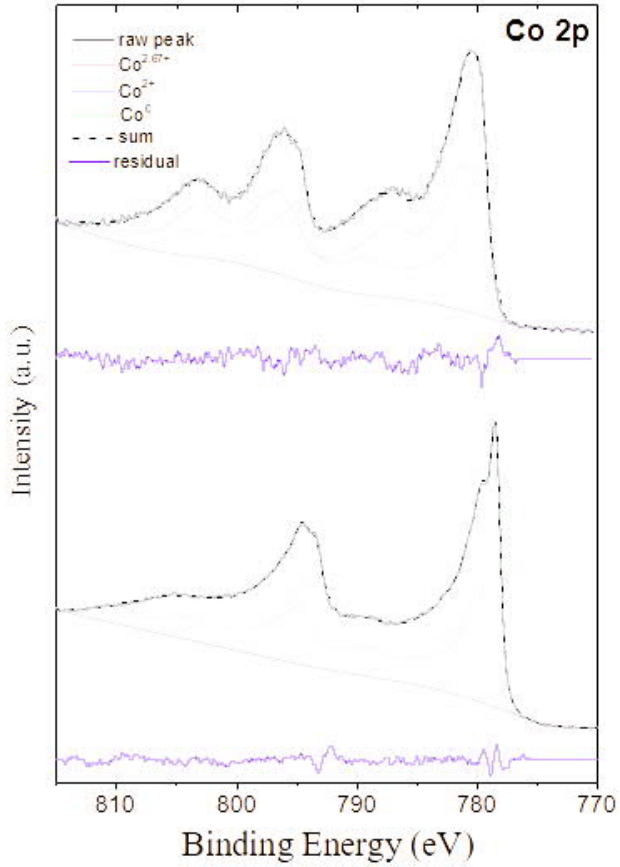


| Peak | FWHM[1] (eV) | **Relative BE shift**[2] (eV) |
|---|---|---|
| $Co^0$ | 1.00±0.05 | 0 |
| CoO | 1.00±0.05 | 1.9±0.2 |
| $Co_3O_4$ | 1.00±0.05 | 1.2±0.2 |

Figure S6: Characteristic examples of Co 2p deconvolution by using reference peak profiles of metallic Co ($Co^0$), CoO ($Co^{2+}$) and $Co_3O_4$ ($Co^{2.67+}$). The table contains parameters and constrains applied to the reference peak line-shapes used for the fitting of Co 2p spectra.

1 The FWHM of the reference component was set as 1.
2 The position of the sharp Co $2p_{3/2}$ component of metallic Co ($Co^0$) at 778.6 eV was used as an internal reference.

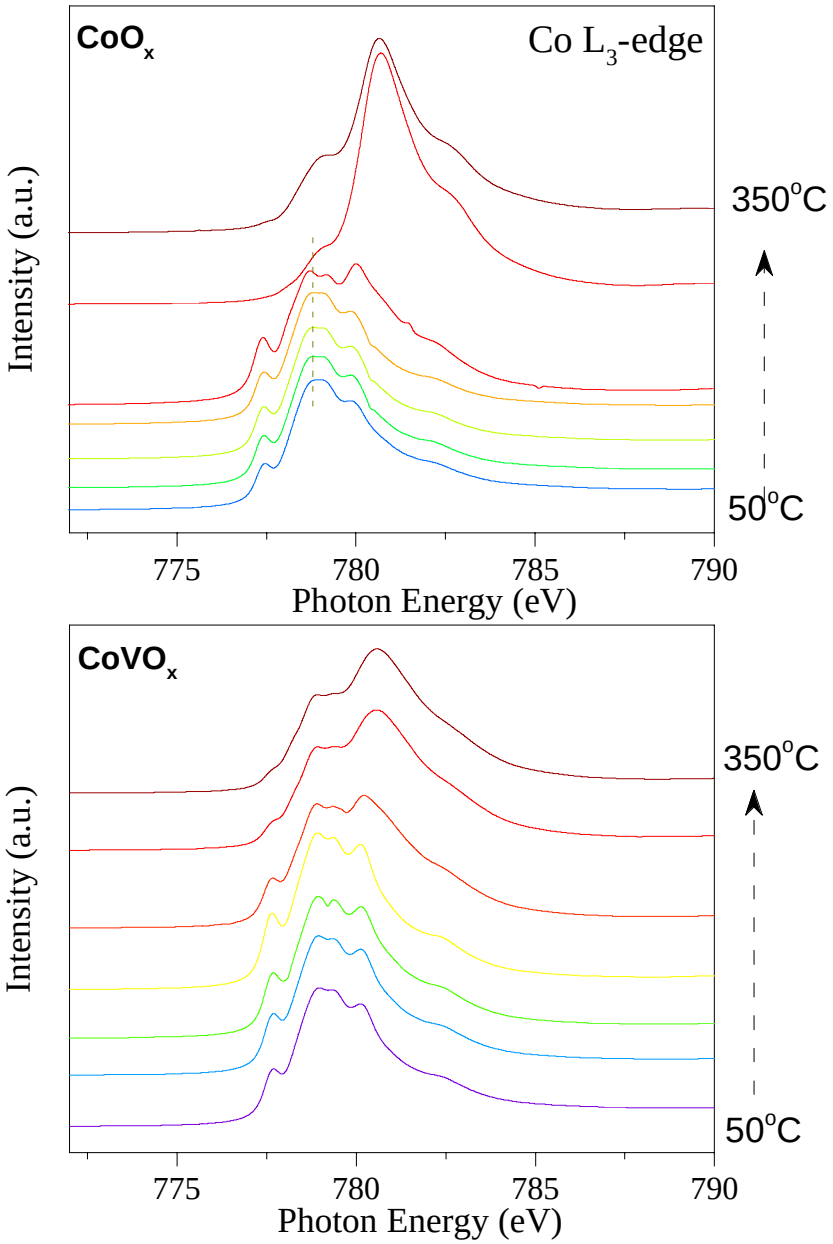


Figure S7: In situ NEXAFS spectra of Co $L_3$-edge over $CoO_x$ *(a)* and $CoVO_x$ *(b)* catalysts recorded at different temperature during COPrOx reaction: 1%CO, 1%$O_2$ and 50%$H_2$ in He, at 0.5mbar total pressure. The spectra are recorded on the Total Electron Yield (TEY) mode. Each spectrum was recorded after about 30 min in the reaction conditions. For clarity all spectra are normalized to the same intensity and offset to the y-axis.

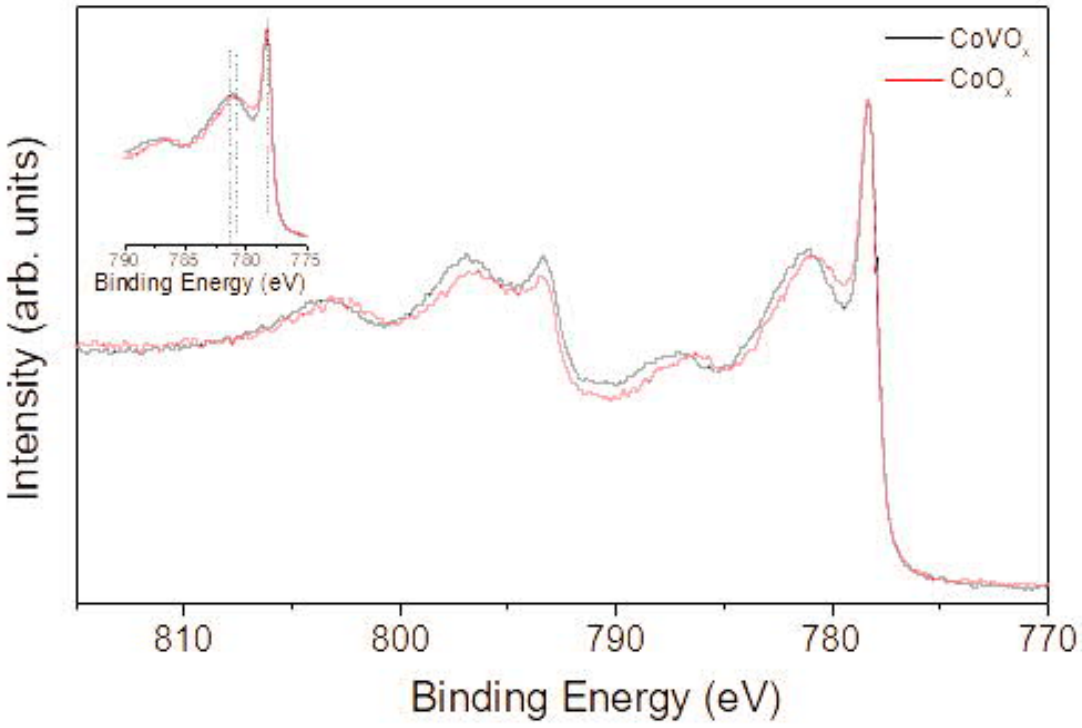


Figure S8: Comparison of the Co 2p spectra of $CoO_x$ (red line) and $CoVO_x$ (black line) catalysts recorded in different reaction conditions but with a very similar cobalt oxidation degree. Both samples demonstrate a characteristic peak at 778.3eV corresponding to $Co^0$. The measurement conditions were: pre-reduction in $H_2$ and measurement under COPrOx mixture at 90 °C for $CoO_x$ and measurement in $H_2$ at 400 °C for $CoVO_x$. The inset focuses on the Co $2p_{3/2}$ peak. For clarity the two spectra are normalized to the same intensity and background.

## Supporting information 9: Depth profile

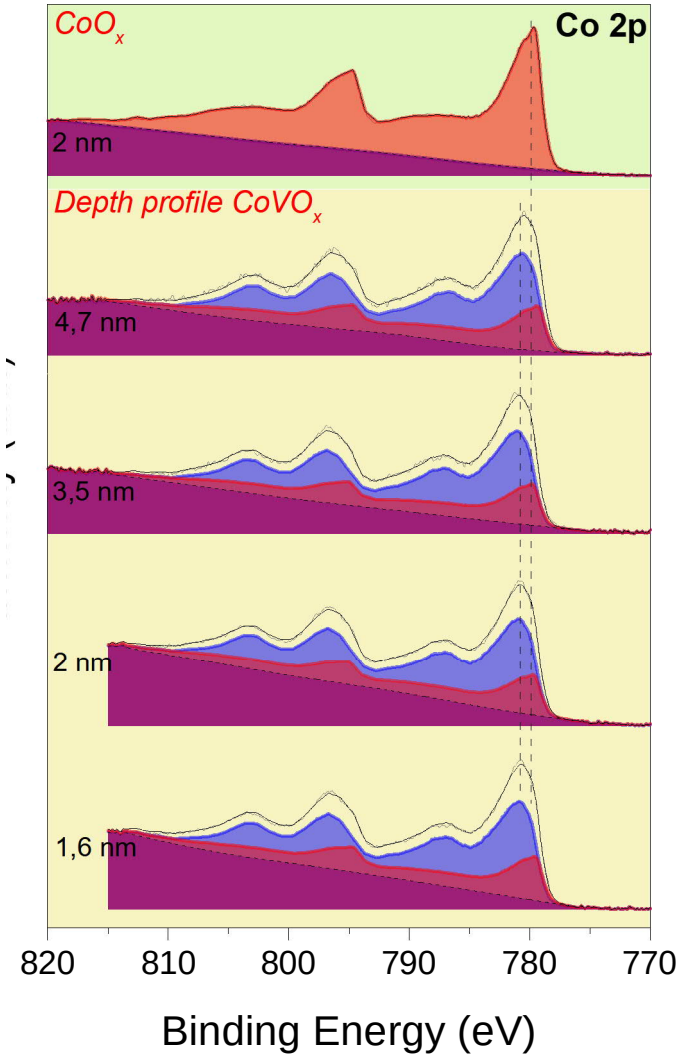


Figure S9. (*bottom part in yellow background*) *In situ* NAP-XPS Co 2p spectra collected over $CoVO_x$ catalyst using four different photon excitation energies (960, 1020, 1340 and 1620 eV) corresponding to Ekin: 180, 240, 560 and 840 eV. The analysis depth of each photon energy was estimated as 3 times the inelastic mean free path. The latter was calculated using the QUASES-IMFP-TPP2M Ver.3.0 software. (*top part in green background*) *Operando* NAP-XPS Co 2p spectra of $CoO_x$ catalyst recorded using excitation photons of 1020 eV. All spectra were recorded at 250 °C in COPrOx reaction conditions. For clarity all spectra are normalized to the same intensity and offset to the y-axis.

## Supporting information 10: V 2p NAP-XPS and V $L_3$-edge NEXAFS

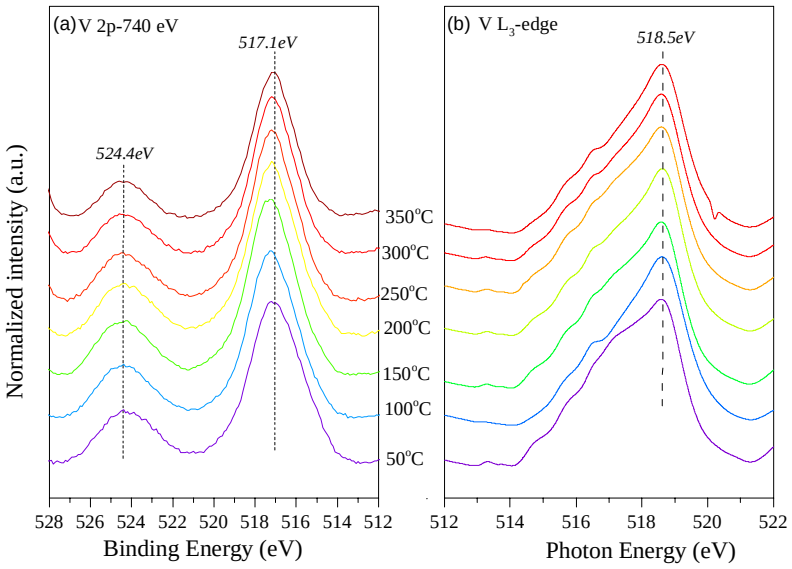


Figure S10. *(a) In situ* V 2p NAP-XPS and *(b)* V $L_3$-edge NEXAFS spectra of $CoVO_x$ catalysts recorded at various temperatures during COPrOx reaction: 1%CO, 1%$O_2$ and 50%$H_2$ in He, at 0.5mbar total pressure. Each spectrum was recorded after about 10 min in the reaction. All spectra recorded above 100°C look quite similar, with several small features visible and the dominant spectra peak positioned at ~518 eV. No shifts are observed with V $L_3$ edge spectra of $CoVO_x$ at different temperature, confirming the XPS results which show that $V^{5+}$ is the dominant oxidation state of vanadium during COPrOx. For clarity all spectra are normalized to the same intensity and offset to the y-axis.

## Supporting information 11: Depth profile

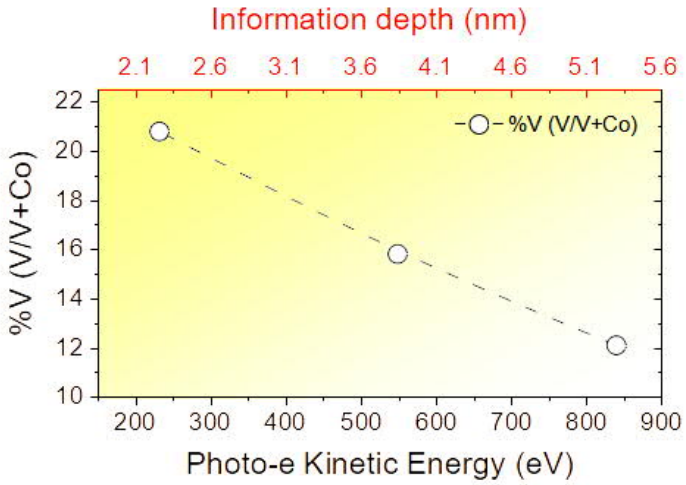


Figure S11. The %at. V as a function of the NAP-XPS analysis depth, calculated from measurements with increasing excitation photon energies. The depth-dependent measurements were recorded at 250 °C in 1%CO, 1%$O_2$ and 50%$H_2$ in He, at 0.5mbar total pressure and correspond to the long-term stability tests.

References

(1) Gao, J.; Wang, Y.; Ping, Y.; Hu, D.; Xu, G.; Gu, F.; Su, F. A Thermodynamic Analysis of Methanation Reactions of Carbon Oxides for the Production of Synthetic Natural Gas. *RSC Adv.* 2012, *2* (6), 2358–2368.

(2) Perkas, N.; Teo, J.; Shen, S.; Wang, Z.; Highfield, J.; Zhong, Z.; Gedanken, A. Supported Ru Catalysts Prepared by Two Sonication-Assisted Methods for Preferential Oxidation of CO in H2. *Phys. Chem. Chem. Phys.* 2011, *13* (34), 15690.

(3) Nyathi, T. M.; Fischer, N.; York, A. P. E.; Morgan, D. J.; Hutchings, G. J.; Gibson, E. K.; Wells, P. P.; Catlow, C. R. A.; Claeys, M. Impact of Nanoparticle-Support Interactions in Co3O4/Al2O3 Catalysts for the Preferential Oxidation of Carbon Monoxide. *ACS Catal.* 2019, *9* (8), 7166–7178.

(4) Jing, P.; Gong, X.; Liu, B.; Zhang, J. Recent Advances in Synergistic Effect Promoted Catalysts for Preferential Oxidation of Carbon Monoxide. *Catal. Sci. Technol.* 2020, *10* (4), 919–934.

(5) Khasu, M.; Nyathi, T.; Morgan, D. J.; Hutchings, G. J.; Claeys, M.; Fischer, N. Co3O4 Morphology in the Preferential Oxidation of CO. *Catal. Sci. Technol.* 2017, *7* (20), 4806–4817.

(6) Gunasooriya, G. T. K. K.; van Bavel, A. P.; Kuipers, H. P. C. E.; Saeys, M. Key Role of Surface Hydroxyl Groups in C–O Activation during Fischer–Tropsch Synthesis. *ACS Catal.* 2016, *6* (6), 3660–3664.

(7) Kersell, H.; Hooshmand, Z.; Yan, G.; Le, D.; Nguyen, H.; Eren, B.; Wu, C. H.; Waluyo, I.; Hunt, A.; Nemšák, S.; Somorjai, G.; Rahman, T. S.; Sautet, P.; Salmeron, M. CO Oxidation Mechanisms on CoOx-Pt Thin Films. *J. Am. Chem. Soc.* 2020, *142* (18), 8312–8322.

(8) Lykhach, Y.; Piccinin, S.; Skála, T.; Bertram, M.; Tsud, N.; Brummel, O.; Farnesi Camellone, M.; Beranová, K.; Neitzel, A.; Fabris, S.; Prince, K. C.; Matolín, V.; Libuda, J. Quantitative Analysis of the Oxidation State of Cobalt Oxides by Resonant Photoemission Spectroscopy. *J. Phys. Chem. Lett.* 2019, *10*, 6129–6136.

(9) Zafeiratos, S.; Dintzer, T.; Teschner, D.; Blume, R.; Hävecker, M.; Knop-Gericke, A.;

Schlögl, R. Methanol Oxidation over Model Cobalt Catalysts: Influence of the Cobalt Oxidation State on the Reactivity. *J. Catal.* 2010, *269* (2), 309–317.

(10) Biesinger, M. C.; Payne, B. P.; Grosvenor, A. P.; Lau, L. W. M.; Gerson, A. R.; Smart, R. S. C. Resolving Surface Chemical States in XPS Analysis of First Row Transition Metals, Oxides and Hydroxides: Cr, Mn, Fe, Co and Ni. *Appl. Surf. Sci.* 2011, *257* (7), 2717–2730.